Cancer Letters 440–441 (2019) 180–188

Contents lists available at ScienceDirect

Cancer Letters

journal homepage: www.elsevier.com/locate/canlet

Original Articles

Transbronchoscopic patient biopsy-derived xenografts as a preclinical model to explore chemorefractory-associated pathways and biomarkers for small-cell lung cancer

Zhijie Wang[a,1], Shuai Fu[b,1], Jun Zhao[c,1], Wei Zhao[d], Zhirong Shen[e], Di Wang[f], Jianchun Duan[a], Hua Bai[a], Rui Wan[a], Jiangyong Yu[a], Shuhang Wang[g], Hanxiao Chen[c], Bolu Chen[h], Lai Wang[e], Jie Wang[a,*]

[a] State Key Laboratory of Molecular Oncology, Department of Medical Oncology, National Cancer Center/Cancer Hospital, Chinese Academy of Medical Sciences & Peking Union Medical College, Beijing, China
[b] Department of Medical Oncology, Shandong Cancer Hospital and Institute, Shandong University, Jinan, China
[c] Department of Thoracic Medical Oncology, Key Laboratory of Carcinogenesis and Translational Research, Peking University Cancer Hospital & Institute, Beijing, China
[d] Department of Cell Biology, Key Laboratory of Carcinogenesis and Translational Research, Peking University Cancer Hospital & Institute, Beijing, China
[e] The BeiGene Pharmaceutical Co. Ltd., Zhongguancun Life Science Park, Beijing, China
[f] Peking-Tsinghua Center for Life Sciences, Academy for Advanced Interdisciplinary Studies, Peking University, Beijing, China
[g] GCP Center, National Cancer Center/Cancer Hospital, Chinese Academy of Medical Sciences & Peking Union Medical College, Beijing, China
[h] CATS Academy Boston, 2001 Washington Street, Braintree, MA, 02184, USA

ARTICLE INFO

Keywords:
Transbronchoscopic patient biopsy-derived xenografts
Chemorefractory
Small-cell lung cancer
Mitogen-activated protein kinase
Receptor tyrosine kinase

ABSTRACT

Insufficient tumor tissue is a major barrier for cancer biology research in small-cell lung cancer (SCLC) and has driven the development of patient-derived xenografts (PDXs) from biopsy tumor tissues. Here, we utilized transbronchoscopic biopsy specimens from SCLC tumors to establish PDXs and evaluated the genomic profile using next-generation sequencing and an RNA sequencing platform. The PDX establishment rate was 54.1% (40/74). PDXs largely recapitulated the major characteristics of their corresponding primary tumors, such as histopathology, genetic profile, and chemo-responsiveness. Compared with chemosensitive (chemo-S) PDXs, chemorefractory (chemo-R) PDXs demonstrated significant gene aberrances in the mitogen-activated protein kinase (MAPK) pathway and a higher frequency of receptor tyrosine kinase (RTK)-related genes. Phosphorylated ERK (pERK) was associated with chemo-R status. Patients with positive pERK expression demonstrated significantly inferior progression-free survival after first-line chemotherapy compared with that of patients who were negative for pERK ($p < 0.001$). Collectively, transbronchoscopic biopsy SCLC PDXs can serve as a model for genomic profiling and identifying biomarkers predictive of chemo-R status. Using PDXs, RTK-related gene aberrances and pERK expression were found to be associated with chemo-R SCLC.

1. Introduction

Small-cell lung cancer (SCLC) accounts for approximately 15% of lung carcinomas and is a highly aggressive malignancy associated with early metastasis, rapid progression, and poor survival [1,2]. Most SCLC patients are diagnosed at a late stage, and systemic drug-dependent therapy is the typical therapeutic strategy. However, efforts to identify and develop novel and effective drugs to treat SCLC have been disappointing, and improvements in survival prognosis have been very limited in recent decades [3,4]. Currently, the most effective strategy is the standard therapy of etoposide plus platinum [5]. Therefore, novel drugs and therapeutic regimens are needed to overcome SCLC. An important challenge in addressing this need is the establishment of suitable models to accurately assess the potential antitumor activity of novel therapies.

At present, the most frequently used *in vivo* models for drug assessment include mice bearing established stable cell lines however, these models fail to mimic complex microenvironments and do not

* Corresponding author. State Key Laboratory of Molecular Oncology, Department of Medical Oncology, National Cancer Center/Cancer Hospital, Chinese Academy of Medical Sciences & Peking Union Medical College, Beijing, 100021, China.
E-mail address: zlhuxi@163.com (J. Wang).
[1] These authors contribute equally to this work.

https://doi.org/10.1016/j.canlet.2018.10.014
Received 30 July 2018; Received in revised form 29 September 2018; Accepted 8 October 2018

effectively reflect tumor heterogeneity [6]. Transgenic mice represent another animal model, but this model is significantly limited by the presence of driver gene aberrations. In response to these deficiencies, patient-derived xenografts (PDXs) have been developed as a possible alternative. To date, PDXs have been successfully established for several cancer types [7], including breast [8–10], gastric [11], colorectal [12,13], lung [14–20], glioma [21] and head and neck [22] cancers. Notably, most PDX models are derived from fresh, surgically resected specimens. Unfortunately, surgical specimen-based PDX models are not suitable for SCLC, which has a low rate of surgical resection. The diagnosis and genetic analysis of SCLC typically rely on small biopsy tumor specimens. This limitation is one of the major barriers that impede a comprehensive understanding of SCLC biology and has motivated the development of biopsied specimen-derived PDXs. These biopsy-directed PDXs can provide a sufficient quantity of fresh tumor tissue for genomic and transcriptomic analyses and create additional opportunities for the assessment of drugs to treat SCLC [18,20].

Despite high response rates to initial chemotherapy, treatment fails to induce a satisfactory improvement in the survival benefits of SCLC patients. The primary potential reason for this phenomenon is the frequent and rapid transition of cancer cells from chemosensitive to chemoresistant phenotypes within 3 months of chemotherapy completion. Moreover, approximately 30% of patients experience disease progression during the initial chemotherapy period. These patients are defined as having chemorefractory (chemo-R) SCLC and frequently face multidrug resistance [23–25]. In this context, the identification of specific biomarkers that are predictive of chemo-R status, which could therefore be used to target biomarker-related signaling pathways beyond chemotherapy, might be a useful strategy. However, no validated effective biomarker has been well established.

Here, we reported the largest series of PDXs established from transbronchial endoscopic biopsies of SCLC tumors to date. We compared the histology, genetic profiles, and chemoresponsiveness of these PDXs with those of their corresponding primary tumors. The disparity in genomic signatures across chemo-R and chemosensitive (chemo-S) SCLC, as well as the chemo-R-associated pathways and biomarkers, were subsequently explored based on the genetic profiles of PDXs examined via targeted next-generation sequencing (NGS) gene panel and RNA sequencing (Seq). The identified biomarker was confirmed in clinical specimens.

2. Materials and methods

2.1. Patient selection and tumor specimen collection

From April 1, 2012, to February 28, 2014, 74 nontreated patients consecutively diagnosed with histologically confirmed SCLC at the Peking University Cancer Hospital were recruited for this study. Patients infected with human immunodeficiency virus (HIV) or hepatitis B/C virus (HBV/HCV) were excluded. All patients underwent transbronchoscopic biopsies and provided written informed consent to donate biopsy tumor tissues for subsequent PDXs. Clinical data for the included patients were collected. The patients with SCLC were sorted into two clinical subtypes: (1) patients with failed first-line chemotherapy ≤ 3 months after platinum-based doublet discontinuation or whose tumor progressed during first-line chemotherapy (chemo-R subtype) and (2) patients who responded to first-line treatment and progressed more than 3 months after the discontinuation of first-line chemotherapy (chemo-S subtype) [24]. This study was approved by the Medical Ethics Committee and Institutional Review Board of the Cancer Hospital Chinese Academy of Medical Sciences & Peking Union Medical College and Peking University Cancer Hospital and was performed in accordance with approved guidelines. All enrolled patients provided informed consent for study analyses.

2.2. PDX establishment

At least two approximately 4-mm^3 fragments of fresh transbronchoscopic biopsies of primary tumors were obtained from each patient. All fragments from patients were transported in ice-cold transport media (10% FBS, Gibco + 1/100 S/P, HyClone + RPMI 1640, HyClone™) at 4 °C and subcutaneously inoculated into the flank of a 6-week-old nonobese diabetic severely combined immunodeficient (NOD/SCID) mouse (Beijing HFK Biotechnology Co., LTD, Beijing, China) within 4–6 h. Tumor volume was measured twice weekly using a Vernier caliper. The tumor volume (v) was calculated according to the formula $v = 0.5 \times (a \times b^2)$, where a and b refer to the longest and shortest diameters of the tumor, respectively. The established PDXs of the initial parental tissue specimens were referred to as passage 1 (P1). When the tumor volume of P1 reached approximately 700 mm^3, the tumor was excised and diced into small fragments (approximately 9 mm^3/fragment) and reimplanted into another mouse to establish subsequent passages, which were referred to as P2, P3, P4, etc. An aliquot of tumor tissue at every passage was frozen in standard cell freezing medium and stored in liquid nitrogen for subsequent propagation, and the remainder of the tumor tissue was preserved for further research. PDXs were considered established if they could be propagated to at least P3 *in vivo*. All procedures were performed under sterile conditions at the SPF facility of BeiGene (Beijing) Co., Ltd. and in accordance with the Guide for the Care and Use of Laboratory Animals of the National Institutes of Health of the United States. These experiments were approved by the Ethics Committee of Animal Experiments of BeiGene Co., Ltd. (Beijing).

2.3. Histopathology assessment

Dried 4-μm slides with formalin-fixed, paraffin-embedded (FFPE) tissues from the parental patient tumors and the PDXs were prepared for hematoxylin-eosin (H&E) and immunohistochemistry (IHC) staining. H&E staining was performed using an H&E staining kit (Applygen, Beijing, China) according to the manufacturer's instructions. IHC staining was performed using specific antibodies, including those targeting CD56 (Cell Signaling Technology, MA, USA), chromogranin A (Santa Cruz Biotechnology, TX, USA), and synaptophysin (Santa Cruz Biotechnology). The phosphorylation status of ERK (pERK) in PDXs and in their corresponding primary tumors was evaluated via IHC staining using an antibody against pERK (Cell Signaling Technology). No staining was observed for the negative controls, which consisted of lung tissue incubated with a nonimmune primary antibody. The H&E and IHC staining assessments were performed by two independent pathologists who were blinded to the sample identity.

2.4. PDX treatment

P4 and subsequent PDX passages were used to evaluate chemoresponsiveness (etoposide plus carboplatin). When the tumor volume reached approximately 200–250 mm^3, the mice were randomized by sequential assignment to either the etoposide plus carboplatin group or the vehicle group. The animals were treated with etoposide and carboplatin as follows:60 mg kg^{-1} carboplatin (Sigma) dissolved in 0.9% saline solution on day 1 and 12 mg kg^{-1} etoposide (Sigma) dissolved in a 12.5:1 0.9% saline:0.1% citric acid solution in 1-methyl-2-pyrrolidinone on days 1–3, or the corresponding vehicle only, each week for a total of 3 weeks. Treatments were administered via oral gavage (p.o.) for vehicle, via intraperitoneal (i.p.) injection for etoposide, or via intravenous injection for carboplatin in a total injection volume of 10 ml/kg body weight. Individual body weight and tumor volume were recorded twice weekly, and the mice were monitored daily for clinical signs of toxicity throughout the duration of the study. When the tumor volume reached 2000 mm^3 or when the tumor was ulcerated, the mice were sacrificed using carbon dioxide.

2.5. Targeted genomics NGS analysis

2.5.1. Genomic DNA extraction, library construction, and sequencing

Genomic DNA was extracted from FFPE or fresh tumor tissues using the QIAamp DNA Mini Kit (Qiagen, Hilden, Germany) according to previously reported methods [26,27]. DNA libraries were prepared using the NEB Next DNA Library Prep Reagent Set (New England BioLabs, MA, USA), followed by Agilent SureSelect^{XT} preps (Agilent, CA, USA). The libraries were sequenced using paired-end 150 bp reads on a HiSeq2500 instrument (Illumina, CA, USA).

2.5.2. Quality control and alignment

Quality control (QC) procedures were performed by cutting adapter sequences, removing low quality reads, and rejecting the reads with a high ratio of 'N' bases. The retained reads were mapped to a human reference (hg19) genome using BWA-MEM, with the following parameters: "-t 10 -k 32" [28]. Duplications were marked with Picard (http://picard.sourceforge.net/index.html).

2.5.3. Variant calling

Somatic single-nucleotide variants (SNVs) and somatic InDels were called using Mutect [29] and Strelka [30], respectively. To improve accuracy, the variant results were filtered using the following procedures: lymphocyte samples were retained if they had mutations in which both allele reads numbered no more than 3 and mutant allele frequencies (MAFs) less than 1%, and tumor samples were retained if the mutations had allele reads numbering greater than 10, MAFs more than 5% and total reads numbering no less than 50 and if the MAF of tumor samples was 10% more than that of matched lymphocyte samples. The genetic annotations were performed with ANNOVAR software [31] and the COSMIC [32] and ClinVar databases.

2.6. Statistical analyses

Statistical analysis was performed using SPSS 23.0 software (SPSS, Chicago, USA). The relationships between clinicopathological characteristics and engraftment rates were analyzed using chi-square tests, unpaired Student's two-tailed t-tests, or one-way analysis of variance (ANOVA). Survival analysis of the PDXs and patients after etoposide plus platinum chemotherapy was performed with Kaplan-Meier curves via log-rank tests. The multivariable Cox proportional hazards model was used for multivariate analysis $p < 0.05$ was considered to indicate significance.

3. Results

3.1. SCLC PDXs preserve the major histological characteristics of the corresponding primary tumors

A total of 74 freshly transbronchoscopic biopsy tumor tissues from SCLC patients were subcutaneously implanted into NOD-SCID mice for PDX establishment. The median age of the 74 patients was 60 years, and the majority of patients were male (53/74, 71.6%). The detailed clinical characteristics of the patients are provided in Table 1. A total of 40 engraftments were passaged beyond P3 (40/74, 54.1%). The success rate of PDX establishment did not significantly correlate with sex, smoking status, disease stage, or clinical subtype (i.e., chemo-S or chemo-R) (Table 1). A total of 33 out of the 74 patients had clinical survival data of first-line chemotherapy (etoposide plus platinum regimen) among these patients, 25 of their associated tumor xenografts were successful with 3 or more passages. The PDX establishment rate was not associated with the progression-free survival (PFS) after first-line chemotherapy [6.6 months (engrafted) *vs.* 6.2 months (unengrafted), $p = 0.87$].

The median duration from initial implantation to P3 establishment (the maximal tumor diameter of the 3rd passage reached 1.5 cm) was 307 days (range, 130–585 days). The median latency periods (from implantation to palpable tumor formation) from initial implantation of the primary tumor fragment to P1, from P1 to P2, and from P2 to P3 were 151 days (range, 81–309 days), 78 days (range, 17–194 days), and 77 days (range, 26–172 days), respectively.

Table 1
Baseline patient characteristics and associations with the establishment rate of transbronchoscopic biopsy PDXs.

Patient characteristics	Patients (N)	Established (n, %)	Nonestablished (n, %)	*p* value
To	74	40 (54)	34 (46)	
Age (median, range)		58 (43–86)	59 (43–81)	
Sex				
Male	53	27 (51)	26 (49)	0.394
Female	21	13 (62)	8 (38)	
Smoking status				
Current/former	47	24 (60)	23 (68)	0.496
Never/light[a]	27	16 (40)	11 (32)	
Disease stage[b]				
Limited	27	15 (43)	12 (44)	0.901
Extensive	35	20 (57)	15 (56)	
Clinical subtype[c]				
Chemosensitive	11	8 (32)	3 (38)	0.774
Chemorefractory	22	17 (68)	5 (62)	

Note: [a] Light smoking was defined as smoking < 100 cigarettes in one's lifetime.
[b, c] A total of 62 patients completed disease staging, and only 33 patients underwent first-line chemotherapy with complete clinical response and survival data.
Abbreviations: PDXs, patient-derived xenografts.

Histopathological comparison between primary tumors and the corresponding xenografts revealed a high degree of similarity (Fig. 1A). Almost all xenografts expressed typical neuroendocrine markers (Syn, CgA, and CD56) in accordance with primary tumors (Fig. 1B) an exception was case Bclu-77, with negative CgA expression in the primary tumor but weak positive expression in the xenograft tissue.

3.2. Responses to chemotherapy of PDXs and their matched primary tumors are concordant

The mice bearing P4 engraftments were used to investigate the concordance of the response to chemotherapy between the primary tumors and the corresponding xenografts (Fig. 1C and D and Supplementary Fig. S1). For example, the representative xenograft (Bclu-04, Fig. 1C) from chemo-S patients exhibited dramatic and persistent tumor regression after treatment with the etoposide plus carboplatin regimen (E/C) and did not demonstrate tumor enlargement until the mice were sacrificed. In contrast, the representative chemo-R xenograft (Bclu-44, Fig. 1D) showed immediate relapse post initial tumor shrinkage after 21 days of chemotherapy treatment. Similarly, the PFS times after first-line E/C chemotherapy of the chemo-R patients were very short (PFS: Bclu-44, 1.5 months Bclu-77, 2.8 months and Bclu-080, 4.9 months) compared with those of the chemo-S patients (PFS: Bclu-04, 9 months Bclu-53, 27.1 months and Bclu-124, 43.5 months.).

3.3. Disparity in gene alteration signatures between chemo-R and chemo-S SCLC

Targeted NGS using a 483-gene panel (Supplementary Table S1) was performed in archival FFPE samples from 8 primary tumors and fresh frozen tumor tissue samples from 20 PDXs, including 9 chemo-S xenografts and 11 chemo-R xenografts according to their corresponding patient primary tumors (Fig. 2). A total of 582 nonsynonymous somatic mutations (362 nonsynonymous SNVs, 22 stop-gain, 11 splice sites, 64 frameshift in/dels and 123 in-frameshift in/dels), 64 gains, and 9 losses

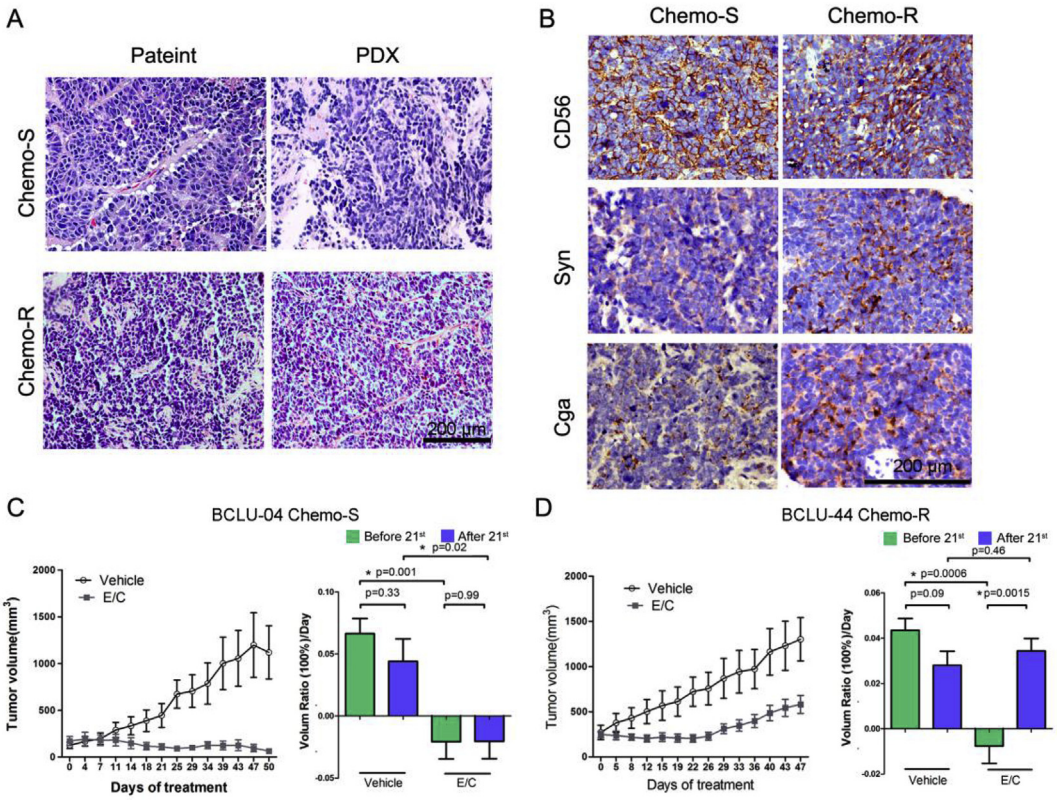

Fig. 1. ***Comparisons of histology and chemo-response between primary tumors and the corresponding PDXs.*** PDXs maintained a high degree of similarity in (A) histopathology and (B) immunohistochemistry with the corresponding primary tumors as indicated in representative chemo-R and chemo-S SCLCs. Comparisons of changing of tumor volumes were compared in PDXs treated by vehicle with chemotherapy in (C) chemo-S and (D) chemo-R SCLCs. Scale bars, 200 μm. SCLC, small-cell lung cancer PDXs, patient-derived xenografts chemo-R, chemorefractory chemo-S, chemosensitive.

were identified based on PDXs. Almost all the gene mutations present in the primary tumors were detected in the corresponding PDXs (median, 85% range, 73–90%). Given the total protein-coding territory of the 483-gene panel of approximately 2.3 Mb, the estimated mean rate of nonsynonymous mutations in chemo-R tumors was 10.2/Mb, which was comparable to that in chemo-S tumors (9.2/Mb). Based on The Cancer Genome Atlas (TCGA) database of SCLC [33,34], the tumor mutational burden (TMB) estimated by the 483-gene panel demonstrated high correlations with whole genome sequencing (WES) data (Supplementary Fig. S2A). According to these data, the estimated TMB values of chemo-S and chemo-R SCLC were comparable (Supplementary Fig. S2B). Additionally, due to the potential effects of DNA damage response (DDR) pathways on TMB, we analyzed the distributions of DDR-related gene mutations and identified similarities between chemo-R and chemo-S SCLC (Supplementary Fig. S2C).

Commonly altered genes (nonsynonymous somatic mutations and/or loss/gain) in SCLC PDXs included *TP53* (80%), *RB1* (70%), *ARID1A* (70%), *KMT2B* (70%), *KMT2D* (35%), *CREBBP* (30%), *KMT2C* (30%) and *CARD11* (30%). None of these gene aberrances exhibited a significantly different distribution between chemo-R and chemo-S SCLC (Fig. 2). C > T/G > A transitions were the most frequent SNVs across chemo-R and chemo-S subtypes (37.4% *vs.* 36.9%, $p = 0.44$ Supplementary Fig. S3A). Generally, similar mutational signatures were observed between these two subtypes. We further compared the distributions of C > T at XpCpG and found that the ratio of Cp(A/C/T) > T was significantly higher in the chemo-R subtype than in the chemo-S subtype (21.3% *vs.* 17.5%, $p = 0.04$ Supplementary Fig. S3B).

To further explore the genetic disparity between chemo-S and chemo-R SCLC, we defined 4 molecular subsets based on the distributions of altered genes (Fig. 2). On the basis of the TCGA database showing that *TP53* and *RB1* aberrances are the invariable signature events in SCLC, we classified *TP53* and *RB1* as “classical SCLC” gene clusters. Gene aberrances whose distributions were similar between chemo-S and chemo-R xenografts were classified as “chemo-S/R shared” gene clusters. Those only observed in chemo-S or chemo-R xenografts were classified as “chemo-S-specific” or “chemo-R-specific” gene clusters, respectively. The most striking finding was that nearly all the cases in the chemo-R group harbored aberrances in receptor tyrosine kinase (RTK)-related genes, which were very limited in the chemo-S group (Fig. 3A and B). However, aberrances in several potentially druggable DDR pathway genes, such as *PARP1*, *PARP2* and *BRCA1,* appeared to be more common in the chemo-S subtype than in the chemo-R subtype. Generally, no differences were observed in drug resistance-related gene aberrances (Fig. 3A, Supplementary Fig. S4), including ATP-binding cassette subfamily C member (ABCC) and low-density lipoprotein-related protein (LRP), and tumor suppressor genes, such as *KMT2* family genes (*KMT2B, KMT2D, KMT2C* and *KMT2A*), across chemo-R and chemo-S SCLC, all of which belonged to the “chemo-S/R shared” gene cluster.

By mapping “chemo-R specific” genes to the Kyoto Encyclopedia of Genes & Genomes (KEGG) pathway database, the MAPK signaling pathway was found to be highly enriched this finding was not observed in the “chemo-S specific” gene cluster. However, other pathways, such as PI3K-AKT-mTOR, ErbB, FoxO and Jak-STAT signaling pathways, were enriched both in chemo-R and chemo-S SCLC (Fig. 3 and Supplementary Fig. S4).

3.4. Distinct profiles of RNA expression in signaling pathway and immunoregulatory genes between chemo-R and chemo-S subtypes

To further identify the key signaling pathways in the chemo-R subtype, RNA Seq was performed to analyze differences in global gene

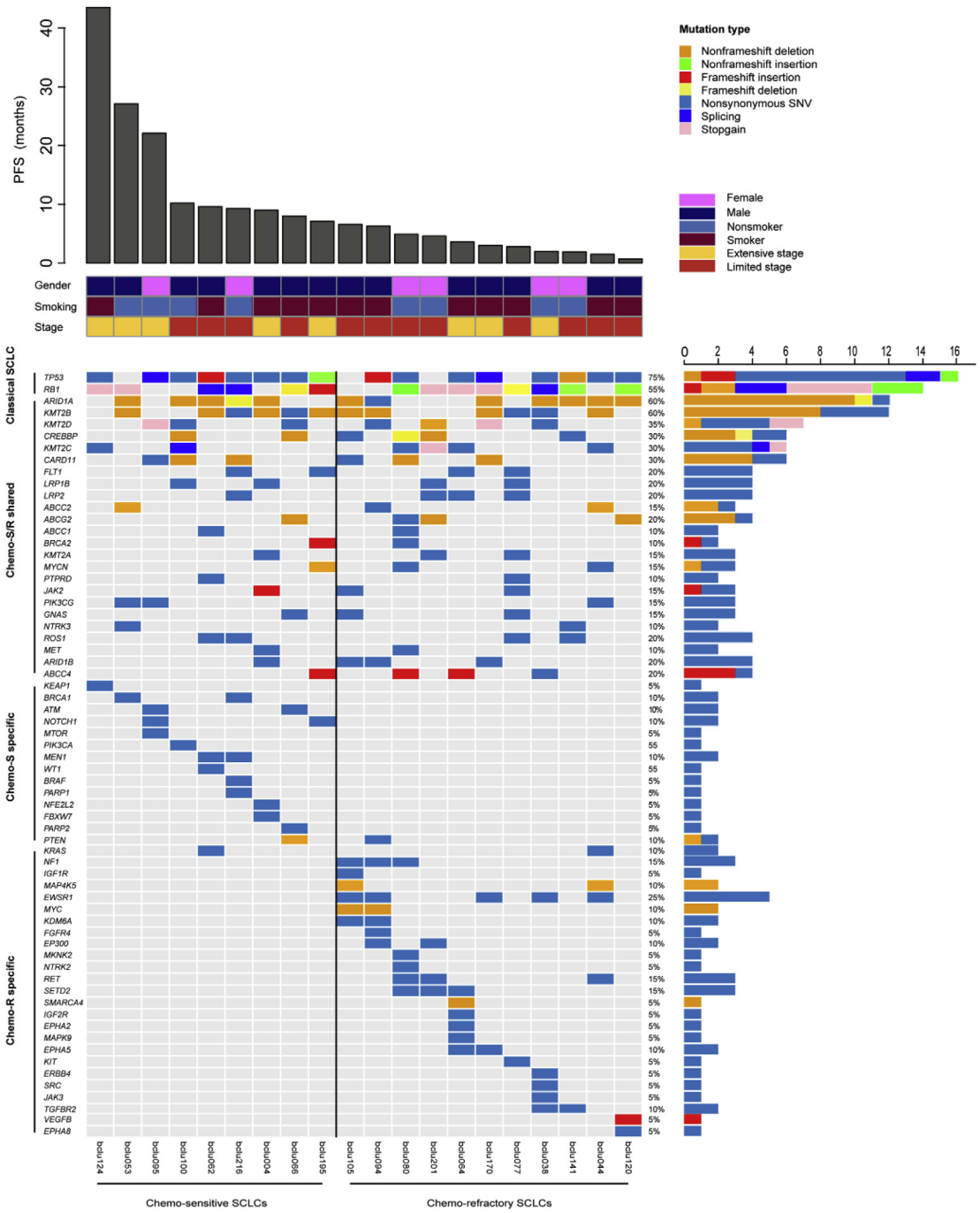

Fig. 2. ***Classification of nonsynonymous somatic mutations based on PDXs.*** Four genetic clusters were identified when PDXs were stratified by chemo-R or chemo-S clinical subtype. The right panel illustrates the frequencies of the somatic mutations. The upper histogram indicates the PFS of each patient, and the lower portion displays their clinical characteristics, including sex, smoking status and disease stage.

expression between chemo-R and chemo-S PDXs. A total of 17 PDXs were used for further gene expression analysis (Supplementary Fig. S5). The genes with distinct expression (with at least 2-fold changes and $p < 0.05$) were extracted and mapped to the KEGG pathway database. Gene enrichments were found in PI3K-AKT-mTOR and MAPK pathways. These pathway-related genes were extracted, and only distinct MAPK pathway-related genes were demonstrated to have a greater tendency toward upregulation in the chemo-R PDXs (Supplementary Fig. S6A) than that of other signaling pathways, such as cell cycle and PI3K-AKT-mTOR pathways.

Previous studies have reported an association of the MAPK pathway with the major histocompatibility complex (MHC) [35,36]. To further investigate the potential influence of the MAPK pathway on the disparity, the differential expression of immune-regulatory genes between these two subtypes was explored (Supplementary Fig. S6B). Human lymphocyte antigen (HLA) class I genes, including *HLA-A*, *HLA-B*, *HLA-C*, *HLA-E*, *HLA-F*, and *HLA-G*, as well as β2 microglobulin (*β2M*), a component of the MHC class I molecule, were expressed at a lower level in chemo-R PDXs than in chemo-S PDXs. Genes involved in effector T cell function (*GNLY*, *IRF1* and *PRF1*), Th1 cell activation (*IL2*, *IL6*, *IL12*A and *IL12RB1*), T cell migration (*CXCL-5*, *CXCL-13*, *CXCR3* and *CCL2*) and costimulating signals (*CD3G*, *CD28* and *CD276*) were upregulated in the chemo-S subtype. Although *CD8B* and *CD4* were highly expressed in the chemo-R subtype, some T cell inhibitors, such as

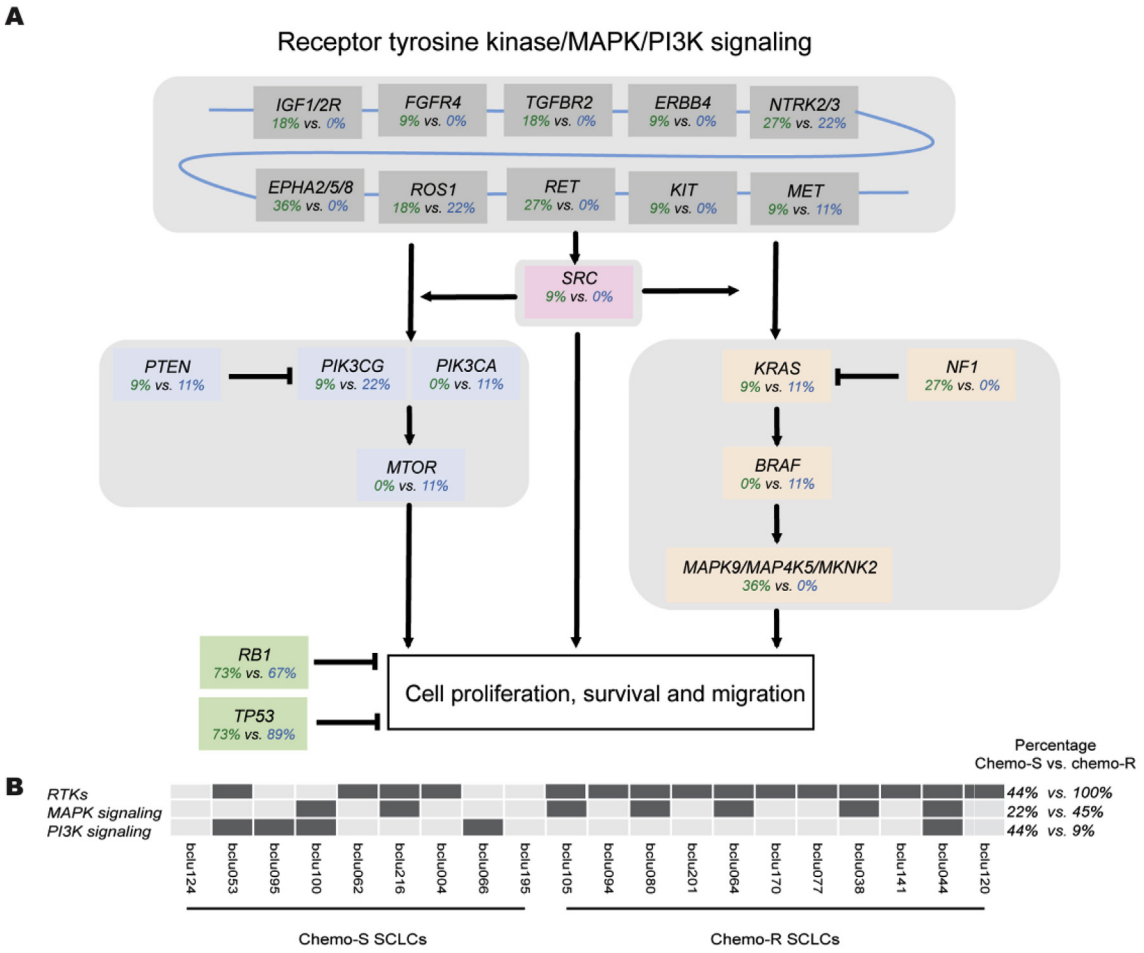

Fig. 3. ***Diagram of integrated lung cancer pathways.*** (A) Proposed diagram of somatic alterations involving key pathway components for RTK, MAPK and PI3K signaling pathways and TP53 and RB1 alterations. Green and blue percentages represent the frequencies of mutations in chemo-R and chemo-S groups, respectively. (B) The distributions of nonsynonymous somatic mutations in chemo-R and chemo-S SCLC. RTK, receptor tyrosine kinase MAPK, mitogen-activated protein kinase PI3K, phosphatidylinositol 3' -kinase. (For interpretation of the references to color in this figure legend, the reader is referred to the Web version of this article.)

FOXP3, *CD69*, *TGFB3* and *IL10,* were also upregulated in the chemo-R subtype. The ligand *PD-L1*, a negative regulator of T cell function, was more highly expressed in the chemo-R group, while the *PD-L2*, *LAG3*, and *PD-L1* regulatory pathway-related genes *STAT3* and *STAT5A* showed relatively elevated levels in the chemo-S group.

3.5. ERK phosphorylation may be a predictive biomarker of chemo-R SCLC

Given the high enrichment of MAPK pathway-related genes in the chemo-R PDXs, a marker that can indicate the activation of the MAPK signaling pathway (e.g., phosphorylated ERK, pERK) was used as a candidate predictor for chemo-R SCLC (Fig. 4A). Ten PDX tumor tissue samples were randomly extracted for pERK IHC staining. All xenografts derived from chemo-R SCLC patients showed positive pERK expression (5/5, 100%), but only 1 of the 5 xenografts derived from the chemo-S SCLC patients was positive for pERK (1/5, 20%, $p = 0.048$, Fig. 4B). To confirm the reproducibility of pERK status as a biomarker in patient samples, the 104 independent cohorts not associated with the initial 10 xenografts underwent IHC staining for pERK. In these 104 clinical samples, chemo-R patients (41/52, 79%) exhibited a higher positive rate for pERK than did chemo-S patients (19/52, 37%, $p < 0.001$, Fig. 4C). Additionally, the PFS of patients positive for pERK after first-line chemotherapy was significantly inferior to that of patients negative for pERK [6 months, 95% confidential interval (CI), 5.2–6.8 months *vs.* 10 months, 95% CI, 7.7–12.3 months, $p < 0.001$, Fig. 4D]. Multivariable Cox proportional hazards model analysis was performed for these factors that included sex (male *vs.* female), age (< 65 years *vs.* ≥ 65 years), smoking status (yes *vs.* no), ECOG performance score (≤1 *vs.* > 1), disease stage (extensive *vs.* limited), and pERK status (positive *vs.* negative). Only pERK level could independently predict poor PFS (hazard ratio = 2.0, 95% CI, 1.3–3.1, $p = 0.003$).

4. Discussion

The results of this study demonstrate that PDXs can be successfully established at a satisfactory rate through the transbronchoscopic biopsy of SCLC tumors and can largely recapitulate the histology, genetic profile, and chemoresponse characteristics of the primary tumor, underlying the feasibility of utilizing these PDXs for preclinical drug assessment. Using a targeted NGS gene panel based on PDXs, chemo-R SCLCs were found to harbor RTK-related gene aberrances more frequently than chemo-S SCLCs, which might be associated with MAPK pathway activation. pERK, as a key member of the MAPK pathway, was found to be a promising biomarker for the prediction of chemorefractory status before initial chemotherapy.

Given the importance of histopathology on guiding subsequent clinical strategy determination and uncommon utilization of surgery to SCLC patients, pathological diagnoses usually rely on transbronchoscopic biopsy, by which, the obtained small tissue samples cannot often be utilized for further molecular analyses and subsequent exploratory research. However, these purposes can be realized through PDX models based on small transbronchoscopic biopsy samples, which can provide

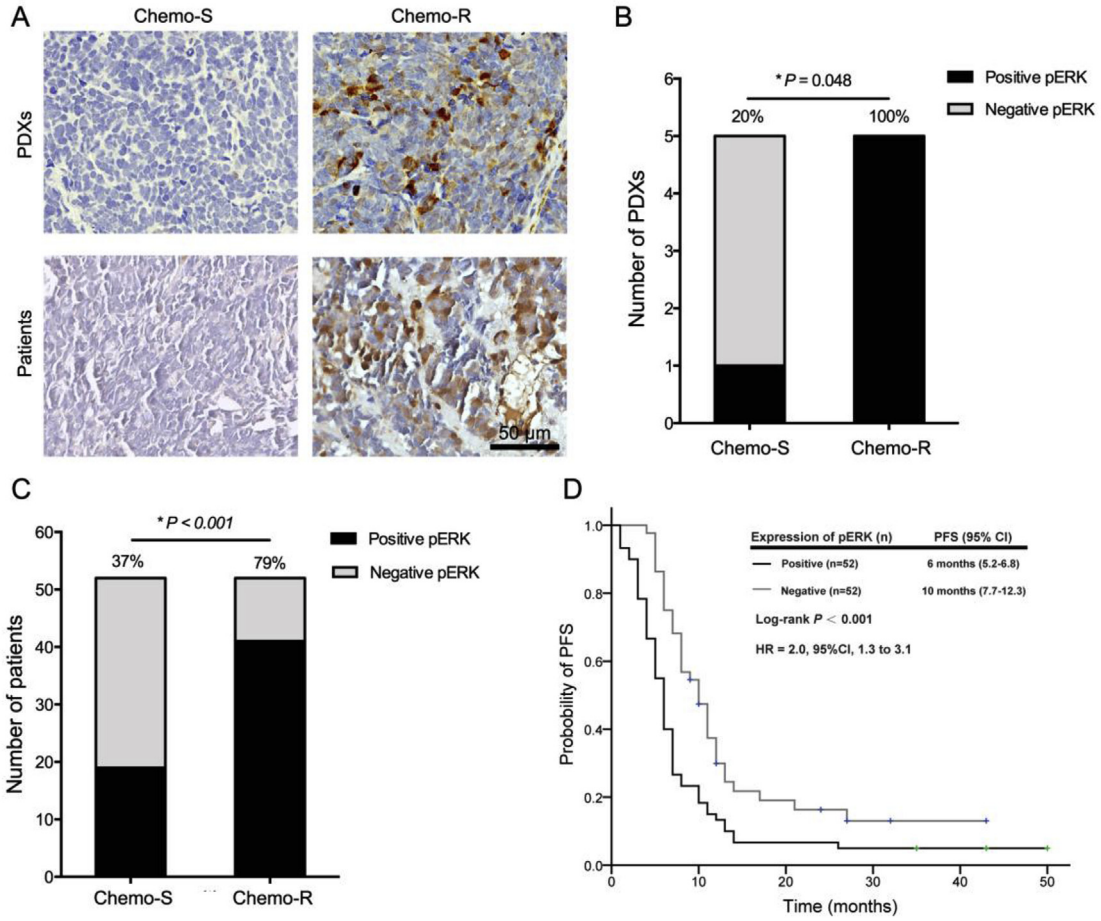

Fig. 4. ***The correlation of pERK expression with SCLC subtype and survival prognosis.*** (A) Representative IHC staining of pERK expression in PDXs and the corresponding primary tumors scale bars, 50 μm. Chemo-R SCLCs demonstrated higher pERK expression than did chemo-S SCLCs in 10 PDXs (B) and 104 unrelated clinical specimens (C). (D) Kaplan-Meier curves of PFS after first-line chemotherapy comparing patients positive and negative for pERK. SCLC, small-cell lung cancer PDXs, patient-derived xenografts PFS, progression-free survival.

sufficient tissues and be extensively used as an available tool for translational research and drug development and assessment. Using small transbronchoscopic biopsy samples, our establishment rate of SCLC PDXs was 54.1%, which was higher than that of most surgery-based PDXs [37–39], although lower than that reported in some previous studies, for example that reported by Leong et al. (10/12 generated first-generation engraftment) [18]. However, not all first-generation engraftments could be passaged further. In our 34 nonestablished SCLC models, 5 cases generated first-generation engrafted tumors but failed in further passages. Moreover, the bias produced by a limited sample size may also have contributed to the observed difference in establishment rates. Generally, NSCLC exhibits a large range of engraftment rates, from 25% to 90% based on surgical specimens [8,14–17]. These results suggest that the establishment rate of PDXs varies in different cancer centers, implying that standard operation procedures need to be built into future protocols. The present study demonstrated that the median latency period from implantation to P1 engraftment was 114 days, similar to that of previously reported PDXs prepared from SCLC biopsy specimens [18] or circulating tumor cells (CTCs) [40]. The shortest latency period from implantation to P3 establishment was 130 days (almost equal to the time course of 4 cycles of initial chemotherapy), indicating that PDXs can potentially be utilized for the effective assessment of drugs beyond first-line platinum-based chemotherapy.

The study reported by Leong et al. demonstrated similar morphological and identical gene mutation profiles between P1 engraftments and patient primary tumors [18]. However, the assessment of heredity from primary tumors to engraftments should be built on the concordance of the primary tumors with not only P1 tumors but also subsequent generations (passages) of engraftments. In the present study, we observed high morphological fidelity during serial passaging (from primary tumor to P1, P2, and P3). Nearly 85% of the gene mutations present in the patient tumors were retained in ≥ P3 engraftments, suggesting the feasibility of using PDXs as the meaningful tools in phenotyping and genotyping assessments. Moreover, our established PDXs recapitulated patient responses to chemotherapy, demonstrating the suitability of these PDXs for use in clinical studies of SCLC biology and as models for drug assessment.

In SCLC, the chemorefractory response to a first-line etoposide plus platinum regimen often indicates multidrug resistance, underscoring the importance of identifying this subtype and exploring novel therapies. However, to date, differentiating chemo-R and chemo-S SCLCs before initial chemotherapy remains difficult. Recently, genomic analyses by Hodgkinson et al. based on CTC-derived xenografts (CDXs) demonstrated that copy number aberration (CNA) gains of several genes, such as *MYCL1, SOX2, BCL2*, and *CCNE1,* were associated with inherent chemotherapy sensitivity [40]. However, only 4 CDXs were used for analysis, and no chemo-R biomarkers were identified, limiting the broad translation of Hodgkinson et al.'s conclusions into clinical practice. By utilizing both PDXs and primary tumor specimens, we found that mutant genes present in chemo-R SCLC were enriched in the MAPK pathway compared with those in chemo-S SCLC. Two further pieces of evidence suggested the activation of the MAPK pathway in chemo-R SCLC. First, the chemorefractory-associated genes were

mainly present in the molecular functions involved in transmembrane RTK and ATP binding, suggesting the tyrosine kinase-directed activation of intracellular signaling pathways and the abnormality of membrane protein drug pumps [41,42]. Second, MAPK pathway activation was indicated by the phosphorylation status of ERK, which was high in chemorefractory SCLC in our study. Our results not only identified pERK as a predictive biomarker of the chemo-R subtype before initial chemotherapy that is convenient for clinical practice but also provided a potential target biomolecule for the development of therapies to reverse chemorefractory status. Obviously, further *in vitro* and *in vivo* experiments are needed to pursue these topics.

One of the problems in SCLC studies is the limited number of tumor specimens available due to biopsy being the primary method of obtaining tumor tissue, thus impeding the launch of further genomic analyses and scientific research. Among our 74 patients, only 8 patients had sufficient tumor tissue for further genetic analyses after the initial H&E and IHC evaluations. However, by establishing PDXs, we obtained sufficient tumor tissue quantities from more than half of the patients. With the exception of *TP53* and *RB1* mutations, we identified several genes primarily found in PDXs but not in the corresponding primary tumors. These results illustrated the advantages of PDXs for genetic analysis compared with those of primary tumors with limited biopsy tissues. In addition, our experiments had several novel and interesting results. RTK-related gene aberrances were more common in chemo-R SCLC than in chemo-S SCLC, suggesting that this SCLC type should be managed distinctly and treated similarly to non-SCLC, and targeted therapies specific to RTKs should be considered. Additionally, chemo-S SCLC appeared to have more significant immunogenicity than chemo-R SCLC, such as an elevated expression of HLA I and effector T cell activation-related genes, as has been previously reported [35,36]. These preliminary results suggested that chemo-S SCLC might be an appropriate candidate for immune therapy. However, future *in vivo* research and clinical studies should be conducted to confirm these results.

Several limitations should be recognized in the present study. The cancer-related gene panel utilized for NGS analyses might raise concerns regarding bias in considering the classification of gene signatures and the corresponding clinical relevance. Thus, alternative theories may explain our findings. Small sample sizes for genetic analyses limit the statistical validity. In this regard, some conclusions from this study should be taken as preliminary evidence and used for the purpose of generating hypotheses that can then be validated in larger basic and clinical studies. However, our findings have some translational relevance and meaningful implications for future potential clinical applications. Further preclinical and clinical interference studies are warranted.

In conclusion, transbronchoscopic biopsy SCLC PDXs can serve as a model for exploring the mechanism underlying chemorefractory responses and depicting the genomic profiling of SCLCs. RTK-related gene aberrances and pERK could potentially predict chemo-R SCLCs, which would facilitate clinical decisions regarding treatment. This finding warrants future prospective studies.

Conflicts of interest

The authors declare that they have no conflict of interest to disclose.

Funding

This work was supported by the National Natural Sciences Foundation Key Program (81630071 and 81330062), National Key R& D Program of China (2016YFC0902300), National High Technology Research and Development Program 863 (SS2015AA020403), CAMS Innovation Fund for Medical Sciences (CIFMS 2016-I2M-3-008), China National Natural Sciences Foundation (81472206 and 81872025), Beijing Natural Science Foundation (7172045), Beijing Nova Program Grants (Z141107001814051), and a grant from Technology Foundation for Selected Oversea Chinese Scholar, Ministry of Human Resources and Social Security of the People's Republic of China in 2014 (to Jun Zhao).

Acknowledgments

We thank the patients and their families, and we thank Novogene Co., Ltd. for their contribution to sequencing analyses.

Abbreviations

SCLC	small-cell lung cancer
PDXs	patient-derived xenografts
MAPK	mitogen-activated protein kinase
DDR	DNA damage response
WES	whole-exome sequencing
SNVs	single-nucleotide variants
RTK	receptor tyrosine kinase
PI3K	phosphatidylinositol 3′ kinase
pERK	phosphorylation of extracellular signal-regulated kinase
PFS	progression-free survival
chemo-S	chemorefractory SCLC
chemo-R	chemosensitive SCLC
NGS	next-generation sequencing
HIV	human immunodeficiency virus
HBV/HCV	hepatitis B/C virus
NOD/SCID	nonobese diabetic severely combined immunodeficient
FFPE	formalin-fixed, paraffin-embedded
H&E	hematoxylin-eosin
IHC	immunohistochemistry
MAFs	mutant allele frequencies
MHC	major histocompatibility complex
HLA	Human lymphocyte antigen
CTCs	circulating tumor cells
CDXs	CTC-derived xenografts
CNA	copy number aberration

Appendix A. Supplementary data

Supplementary data to this article can be found online at https://doi.org/10.1016/j.canlet.2018.10.014.

References

[1] B.I. Gustafsson, M. Kidd, A. Chan, M.V. Malfertheiner, M. Modlin, Bronchopulmonary neuroendocrine tumors, Cancer 113 (1) (2008) 5–21.
[2] W.D. Travis, Lung tumours with neuroendocrine differentiation, Eur. J. Canc. 45 (Suppl 1) (2009) 251–266.
[3] S.M. Gadgeel, Targeted therapy and immune therapy for small cell lung cancer, Curr. Treat. Options Oncol. 19 (11) (2018) 53.
[4] Y.K. Chae, A. Pan, A.A. Davis, N. Mohindra, M. Matsangou, V. Villaflor, F. Giles, Recent advances and future strategies for immune-checkpoint inhibition in small-cell lung cancer, Clin. Lung Canc. 18 (2) (2017) 132–140.
[5] W.N. William Jr., B.S. Glisson, Novel strategies for the treatment of small-cell lung carcinoma, Nat. Rev. Clin. Oncol. 8 (10) (2011) 611–619.
[6] M. Suggitt, M.C. Bibby, 50 years of preclinical anticancer drug screening: empirical to target-driven approaches, Clin. Canc. Res. 11 (3) (2005) 971–981.
[7] D. Siolas, G.J. Hannon, Patient-derived tumor xenografts: transforming clinical samples into mouse models, Cancer Res. 73 (17) (2013) 5315–5319.
[8] Y.S. DeRose, G. Wang, Y.C. Lin, J.T. Rhodes, W.L. Devereux, C.M. Rudin, R. Yung, G. Parmigiani, M. Dorsch, C.D. Peacock, D.N. Watkins, Tumor grafts derived from women with breast cancer authentically reflect tumor pathology, growth, metastasis and disease outcomes, Nat. Med. 17 (8) (2011) 1514–1520.
[9] E. Marangoni, A. Vincent-Salomon, N. Auger, A. Degeorges, F. Assayag, P. de Cremoux, L. de Plater, C. Guyader, G. De Pinieux, J.G. Judde, M. Rebucci, C. Tran-Perennou, X. Sastre-Garau, B. Sigal-Zafrani, O. Delattre, V. Diéras, M.F. Poupon, A new model of patient tumor-derived breast cancer xenografts for preclinical assays, Clin. Canc. Res. 13 (13) (2007) 3989–3998.
[10] R.R. Rosato, D. Dávila-González, D.S. Choi, W. Qian, W. Chen, A.J. Kozielski, H. Wong, B. Dave, J.C. Chang, Evaluation of anti-PD-1-based therapy against triple-negative breast cancer patient-derived xenograft tumors engrafted in humanized mouse models, Breast Cancer Res. 20 (1) (2018) 108.
[11] Y. Zhu, T. Tian, Z. Li, Z. Tang, L. Wang, J. Wu, Y. Li, B. Dong, Y. Li, N. Li, J. Zou,

J. Gao, L. Shen, Establishment and characterization of patient-derived tumor xenograft using gastroscopic biopsies in gastric cancer, Sci. Rep. 5 (2015) 8542.
[12] M. Linnebacher, C. Maletzki, C. Ostwald, U. Klier, M. Krohn, E. Klar, F. Prall, Cryopreservation of human colorectal carcinomas prior to xenografting, BMC Canc. 10 (2010) 362.
[13] A. Spreafico, J.J. Tentler, T.M. Pitts, A.C. Tan, M.A. Gregory, J.J. Arcaroli, P.J. Klauck, M.C. McManus, R.J. Hansen, J. Kim, L.N. Micel, H.M. Selby, T.P. Newton, K.L. McPhillips, D.L. Gustafson, J.V. Degregori, W.A. Messersmith, R.A. Winn, S.G. Eckhardt, Rational combination of a MEK inhibitor, selumetinib, and the Wnt/calcium pathway modulator, cyclosporin A, in preclinical models of colorectal cancer, Clin. Canc. Res. 19 (15) (2013) 4149–4162.
[14] J.C. Cutz, J. Guan, J. Bayani, M. Yoshimoto, H. Xue, M. Sutcliffe, J. English, J. Flint, J. LeRiche, J. Yee, J.A. Squire, P.W. Gout, S. Lam, Y.Z. Wang, Establishment in severe combined immunodeficiency mice of subrenal capsule xenografts and transplantable tumor lines from a variety of primary human lung cancers: potential models for studying tumor progression-related changes, Clin. Canc. Res. 12 (13) (2006) 4043–4054.
[15] I. Fichtner, J. Rolff, R. Soong, J. Hoffmann, S. Hammer, A. Sommer, M. Becker, J. Merk, Establishment of patient-derived non-small cell lung cancer xenografts as models for the identification of predictive biomarkers, Clin. Canc. Res. 14 (20) (2008) 6456–6468.
[16] E.L. Stewart, C. Mascaux, N.A. Pham, S. Sakashita, J. Sykes, L. Kim, N. Yanagawa, G. Allo, K. Ishizawa, D. Wang, C.Q. Zhu, M. Li, C. Ng, N. Liu, M. Pintilie, P. Martin, T. John, I. Jurisica, N.B. Leighl, B.G. Neel, T.K. Waddell, F.A. Shepherd, G. Liu, M.S. Tsao, Clinical utility of patient-derived xenografts to determine biomarkers of prognosis and map resistance pathways in EGFR-mutant lung adenocarcinoma, J. Clin. Oncol. 33 (22) (2015) 2472–2480.
[17] J. Merk, J. Rolff, M. Becker, G. Leschber, I. Fichtner, Patient-derived xenografts of non-small-cell lung cancer: a pre-clinical model to evaluate adjuvant chemotherapy? Eur. J. Cardio. Thorac. Surg. 36 (3) (2009) 454–459.
[18] T.L. Leong, K.D. Marini, F.J. Rossello, S.N. Jayasekara, P.A. Russell, Z. Prodanovic, B. Kumar, V. Ganju, M. Alamgeer, L.B. Irving, D.P. Steinfort, C.D. Peacock, J.E. Cain, A. Szczepny, D.N. Watkins, Genomic characterisation of small cell lung cancer patient-derived xenografts generated from endobronchial ultrasound-guided transbronchial needle aspiration specimens, PLoS One 9 (9) (2014) e106862.
[19] V.C. Daniel, L. Marchionni, J.S. Hierman, et al., A primary xenograft model of small-cell lung cancer reveals irreversible changes in gene expression imposed by culture in vitro, Cancer Res. 69 (2009) 3364–3373.
[20] B.J. Drapkin, J. George, C.L. Christensen, M. Mino-Kenudson, R. Dries, T. Sundaresan, S. Phat, D.T. Myers, J. Zhong, P. Igo, M.H. Hazar-Rethinam, J.A. Licausi, M. Gomez-Caraballo, M. Kem, K.N. Jani, R. Azimi, N. Abedpour, R. Menon, S. Lakis, R.S. Heist, R. Büttner, S. Haas, L.V. Sequist, A.T. Shaw, K.K. Wong, A.N. Hata, M. Toner, S. Maheswaran, D.A. Haber, M. Peifer, N. Dyson, R.K. Thomas, A.F. Farago, Genomic and functional fidelity of small cell lung cancer patient-derived xenografts, Cancer Discov. 8 (5) (2018) 600–615.
[21] P.C. De Witt Hamer, A.A. Van Tilborg, P.P. Eijk, P. Sminia, D. Troost, C.J. Van Noorden, B. Ylstra, S. Leenstra, The genomic profile of human malignant glioma is altered early in primary cell culture and preserved in spheroids, Oncogene 27 (14) (2008) 2091–2096.
[22] K. Nitschinsk, A. Idris, N. McMillan, Patient derived xenografts as models for head and neck cancer, Cancer Lett. 434 (2018) 114–119.
[23] J.P. van Meerbeeck, D.A. Fennell, D.K. De Ruysscher, Small-cell lung cancer, Lancet 378 (9804) (2011) 1741–1755.
[24] A. Ardizzoni, H. Hansen, P. Dombernowsky, T. Gamucci, S. Kaplan, P. Postmus, G. Giaccone, B. Schaefer, J. Wanders, J. Verweij, Topotecan, a new active drug in the second-line treatment of small-cell lung cancer: a phase II study in patients with refractory and sensitive disease. The european organization for research and treatment of cancer early clinical studies group and new drug development office, and the lung cancer cooperative group, J. Clin. Oncol. 15 (5) (1997) 2090–2096.
[25] T.S.M. Ciuleanu, Y. Demidchik, et al., Randomized phase III study (SPEAR) of picoplatin plus best supportive care (BSC) or BSC alone in patients (pts) with SCLC refractory or progressive within 6 months after first-line platinum-based chemotherapy, J. Clin. Oncol. 28 (15 suppl) (2010) 7002.
[26] H. Bai, L. Mao, H.S. Wang, J. Zhao, L. Yang, T.T. An, X. Wang, C.J. Duan, N.M. Wu, Z.Q. Guo, Y.X. Liu, H.N. Liu, Y.Y. Wang, J. Wang, Epidermal growth factor receptor mutations in plasma DNA samples predict tumor response in Chinese patients with stages IIIB to IV non-small-cell lung cancer, J. Clin. Oncol. 27 (16) (2009) 2653–2659.
[27] H. Bai, Z. Wang, K. Chen, J. Zhao, J.J. Lee, S. Wang, Q. Zhou, M. Zhuo, L. Mao, T. An, J. Duan, L. Yang, M. Wu, Z. Liang, Y. Wang, X. Kang, J. Wang, Influence of chemotherapy on EGFR mutation status among patients with non-small-cell lung cancer, J. Clin. Oncol. 30 (25) (2012) 3077–3083.
[28] H. Li, R. Durbin, Fast and accurate short read alignment with Burrows-Wheeler transform, Bioinformatics 25 (14) (2009) 1754–1760.
[29] K. Cibulskis, M.S. Lawrence, S.L. Carter, A. Sivachenko, D. Jaffe, C. Sougnez, S. Gabriel, M. Meyerson, E.S. Lander, G. Getz, Sensitive detection of somatic point mutations in impure and heterogeneous cancer samples, Nat. Biotechnol. 31 (3) (2013) 213–219.
[30] C.T. Saunders, W.S. Wong, S. Swamy, J. Becq, L.J. Murray, R.K. Cheetham, Strelka: accurate somatic small-variant calling from sequenced tumor-normal sample pairs, Bioinformatics 28 (14) (2012) 1811–1817.
[31] K. Wang, M. Li, H. Hakonarson, ANNOVAR: functional annotation of genetic variants from high-throughput sequencing data, Nucleic Acids Res. 38 (16) (2010) e164.
[32] S.A. Forbes, G. Tang, N. Bindal, S. Bamford, E. Dawson, C. Cole, C.Y. Kok, M. Jia, R. Ewing, A. Menzies, J.W. Teague, M.R. Stratton, P.A. Futreal, COSMIC (the Catalogue of Somatic Mutations in Cancer): a resource to investigate acquired mutations in human cancer, Nucleic Acids Res. 38 (Database issue) (2010) D652–D765.
[33] J. George, J.S. Lim, S.J. Jand, Y. Cun, L. Ozretić, G. Kong, F. Leenders, X. Lu, L. Fernández-Cuesta, G. Bosco, C. Müller, I. Dahmen, N.S. Jahchan, K.S. Park, D. Yang, A.N. Karnezis, D. Vaka, A. Torres, M.S. Wang, J.O. Korbel, R. Menon, S.M. Chun, D. Kim, M. Wilkerson, N. Hayes, D. Engelmann, B. Pützer, M. Bos, S. Michels, I. Vlasic, D. Seidel, B. Pinther, P. Schaub, C. Becker, J. Altmüller, J. Yokota, T. Kohno, R. Iwakawa, K. Tsuta, M. Noguchi, T. Muley, H. Hoffmann, P.A. Schnabel, I. Petersen, Y. Chen, A. Soltermann, V. Tischler, C.M. Choi, Y.H. Kim, P.P. Massion, Y. Zou, D. Jovanovic, M. Kontic, G.M. Wright, P.A. Russell, B. Solomon, I. Koch, M. Lindner, L.A. Muscarella, A. la Torre, J.K. Field, M. Jakopovic, J. Knezevic, E. Castaños-Vélez, L. Roz, U. Pastorino, O.T. Brustugun, M. Lund-Iversen, E. Thunnissen, J. Köhler, M. Schuler, J. Botling, M. Sandelin, M. Sanchez-Cespedes, H.B. Salvesen, V. Achter, U. Lang, M. Bogus, P.M. Schneider, T. Zander, S. Ansén, M. Hallek, J. Wolf, M. Vingron, Y. Yatabe, W.D. Travis, P. Nürnberg, C. Reinhardt, S. Perner, L. Heukamp, R. Büttner, S.A. Haas, E. Brambilla, M. Peifer, J. Sage, R.K. Thomas, Comprehensive genomic profiles of small cell lung cancer, Nature (2015) 47–53.
[34] M. Peifer, L. Fernandez-Cuesta, M.L. Sos, J. George, D. Seidel, L.H. Kasper, D. Plenker, F. Leenders, R. Sun, T. Zander, R. Menon, M. Koker, I. Dahmen, C. Müller, V. Di Cerbo, H.U. Schildhaus, J. Altmüller, I. Baessmann, C. Becker, B. de Wilde, J. Vandesompele, D. Böhm, S. Ansén, F. Gabler, I. Wilkening, S. Heynck, J.M. Heuckmann, X. Lu, S.L. Carter, K. Cibulskis, S. Banerji, G. Getz, K.S. Park, D. Rauh, C. Grütter, M. Fischer, L. Pasqualucci, G. Wright, Z. Wainer, P. Russell, I. Petersen, Y. Chen, E. Stoelben, C. Ludwig, P. Schnabel, H. Hoffmann, T. Muley, M. Brockmann, W. Engel-Riedel, L.A. Muscarella, V.M. Fazio, H. Groen, W. Timens, H. Sietsma, E. Thunnissen, E. Smit, D.A. Heideman, P.J. Snijders, F. Cappuzzo, C. Ligorio, S. Damiani, J. Field, S. Solberg, O.T. Brustugun, M. Lund-Iversen, J. Sänger, J.H. Clement, A. Soltermann, H. Moch, W. Weder, B. Solomon, J.C. Soria, P. Validire, B. Besse, E. Brambilla, C. Brambilla, S. Lantuejoul, P. Lorimier, P.M. Schneider, M. Hallek, W. Pao, M. Meyerson, J. Sage, J. Shendure, R. Schneider, R. Büttner, J. Wolf, P. Nürnberg, S. Perner, L.C. Heukamp, P.K. Brindle, S. Haas, R.K. Thomas, Integrative genome analyses identify key somatic driver mutations of small-cell lung cancer, Nat. Genet. (2012) 1104–1110.
[35] E.J. Brea, C.Y. Oh, E. Manchado, S. Budhu, R.S. Gejman, G. Mo, P. Mondello, J.E. Han, C.A. Jarvis, D. Ulmert, Q. Xiang, A.Y. Chang, R.J. Garippa, T. Merghoub, J.D. Wolchok, N. Rosen, S.W. Lowe, D.A. Scheinberg, Kinase regulation of human MHC class I molecule expression on cancer cells, Canc. Immunol. Res. 4 (11) (2016) 936–947.
[36] S. Hu-Lieskovan, S. Mok, B. Homet Moreno, J. Tsoi, L. Robert, L. Goedert, E.M. Pinheiro, R.C. Koya, T.G. Graeber, B. Comin-Anduix, A. Ribas, Improved antitumor activity of immunotherapy with BRAF and MEK inhibitors in BRAF(V600E) melanoma, Sci. Transl. Med. 7 (279) (2015) 279ra41.
[37] C. Hao, L. Wang, S. Peng, M. Cao, H. Li, J. Hu, X. Huang, W. Liu, H. Zhang, S. Wu, A. Pataer, J.V. Heymach, A.K. Eterovic, Q. Zhang, K.R. Shaw, K. Chen, A. Futreal, M. Wang, W. Hofstetter, R. Mehran, D. Rice, J.A. Roth, B. Sepesi, S.G. Swisher, A. Vaporciyan, G.L. Walsh, F.M. Johnson, B. Fang, Gene mutations in primary tumors and corresponding patient-derived xenografts derived from non-small cell lung cancer, Cancer Lett. 357 (1) (2015) 179–185.
[38] M. Massimo, B. Giulia, C. Roberto, C. Borzi, M. Boeri, A. Fabbri, G. Leone, P. Gasparini, C. Galeone, G. Pelosi, L. Roz, G. Sozzi, U. Pastorino, Establishment of patient derived xenografts as functional testing of lung cancer aggressiveness, Sci. Rep. 7 (1) (2017) 6689.
[39] D. Roife, Y. Kang, L. Wang, B. Fang, S.G. Swisher, J.E. Gershenwald, S. Pretzsch, C.P. Dinney, M.H.G. Katz, J.B. Fleming, Generation of patient-derived xenografts from fine needle aspirates or core needle biopsy, Surgery 161 (5) (2017) 1246–1254.
[40] C.L. Hodgkinson, C.J. Morrow, Y. Li, R.L. Metcalf, D.G. Rothwell, F. Trapani, R. Polanski, D.J. Burt, K.L. Simpson, K. Morris, S.D. Pepper, D. Nonaka, A. Greystoke, P. Kelly, B. Bola, M.G. Krebs, J. Antonello, M. Ayub, S. Faulkner, L. Priest, L. Carter, C. Tate, C.J. Miller, F. Blackhall, G. Brady, C. Dive, Tumorigenicity and genetic profiling of circulating tumor cells in small-cell lung cancer, Nat. Med. 20 (8) (2014) 897–903.
[41] H. Ying, A.C. Kimmelman, C.A. Lyssiotis, S. Hua, G.C. Chu, E. Fletcher-Sananikone, J.W. Locasale, J. Son, H. Zhang, J.L. Coloff, H. Yan, W. Wang, S. Chen, A. Viale, H. Zheng, J.H. Paik, C. Lim, A.R. Guimaraes, E.S. Martin, J. Chang, A.F. Hezel, S.R. Perry, J. Hu, B. Gan, Y. Xiao, J.M. Asara, R. Weissleder, Y.A. Wang, L. Chin, L.C. Cantley, R.A. DePinho, Oncogenic Kras maintains pancreatic tumors through regulation of anabolic glucose metabolism, Cell 149 (3) (2012) 656–670.
[42] J.J. Yeh, N.Y. Hsu, W.H. Hsu, C.H. Tsai, C.C. Lin, J.A. Liang, Comparison of chemotherapy response with P-glycoprotein, multidrug resistance-related protein-1, and lung resistance-related protein expression in untreated small cell lung cancer, Lung 183 (3) (2005) 177–183.